

# Voltammetric Studies with Adhered Microparticles and the Detection of a Dependence of Organometallic $\text{Cis}^+ \rightarrow \text{Trans}^+$ First-Order Isomerization Rate Constants on the Identity of the Ionic Liquid

Jie Zhang and Alan M. Bond\*

School of Chemistry, Monash University, Clayton, Victoria 3800, Australia

Received: February 17, 2004; In Final Form: March 11, 2004

Voltammetric studies employing electrode surfaces modified with microparticles of redox active solid can be used conveniently to obtain thermodynamic and kinetic information in ionic liquids in cases where a first-order chemical reaction of rapidly dissolved electrolyzed product is coupled to the electron-transfer process. Experimental and theoretical verification of this concept is provided. A study based on the voltammetric oxidation of durene (*J. Phys. Chem. A* **2003**, *107*, 745) to its cation radical contains a first-order followup chemical reaction that is almost independent of whether organic solvent (electrolyte) or ionic liquid media are used. In contrast, it has now been found that the rate constants ( $k_f$ ) for the first-order  $\text{cis}^+ \rightarrow \text{trans}^+$  isomerization reactions that accompany the one-electron oxidation of microparticles of the organometallic compounds *cis*-[Mn(CN)(CO)<sub>2</sub>{P(OPh)<sub>3</sub>}(DPM)] (DPM = Ph<sub>2</sub>PCH<sub>2</sub>PPh<sub>2</sub>) or *cis*-[W(CO)<sub>2</sub>(DPE)<sub>2</sub>] (DPE = Ph<sub>2</sub>PCH<sub>2</sub>CH<sub>2</sub>PPh<sub>2</sub>) depend significantly on the identity of the ionic liquid. In the case of trihexyl(tetradecyl)-phosphonium tris(pentafluoroethyl)trifluorophosphate ionic liquid,  $k_f$  is similar to the value found in conventional organic solvent (electrolyte) media, but significantly faster than that in the ionic liquids, 1-butyl-3-methylimidazolium hexafluorophosphate, (1-ethyl-3-methylimidazolium)bis[(trifluoromethyl)sulfonyl]amide, and (*N*-butyl-*N*-methylpyrrolidinium)bis[(trifluoromethyl)sulfonyl]amide. No simple correlation of  $k_f$  values with the physical or chemical properties of these ionic liquids has been elucidated.

## Introduction

Ionic liquids are being widely employed in many branches of chemistry because of their advantageous properties, such as, negligible vapor pressure, low toxicity, high chemical, electrochemical and thermal stability, high conductivity, and the ability to dissolve a wide range of organic and inorganic compounds.<sup>1–3</sup>

The majority of a now extensive series of reports of electrochemical studies in ionic liquids have been directed toward establishment of the potential windows of the ionic liquids,<sup>1</sup> studies of metal stripping/deposition process,<sup>1c</sup> and measurements of reversible potentials.<sup>4</sup> Surprisingly, relatively few studies have been carried out to investigate the chemical reactivity of species that have been electrochemically generated in ionic liquids other than in the case of haloaluminate molten salts.<sup>5</sup> Recent quantitative studies by Hapiot and co-workers,<sup>6</sup> who described the reactivity of a range of electrogenerated species a range of ionic liquids containing 1-alkyl-3-methylimidazolium or quaternary ammonium cations (with PF<sub>6</sub><sup>−</sup> or N(SO<sub>2</sub>CF<sub>3</sub>)<sub>2</sub><sup>−</sup> as counteranions), is one of the notable exceptions. In this voltammetric study, undertaken in both ionic liquids and acetonitrile (0.2 M Et<sub>4</sub>NPF<sub>6</sub>), durene was oxidized to its radical cation, which was then followed by a first-order process to form a neutral radical. Intriguingly, the kinetics of the first-order homogeneous chemical reaction coupled to the electron-transfer step (first-order EC reaction scheme<sup>7</sup>) was not significantly influenced by the use of an ionic liquid as an alternative to a conventional organic (electrolyte) medium. In contrast, the kinetics of second-order homogeneous chemical reactions coupled to electron transfer were affected due to the slower

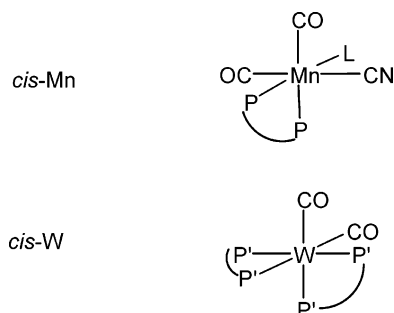
diffusion kinetics in the highly viscous ionic liquids. The chemical reactivity of electrogenerated superoxide in the ionic liquid, 1-butyl-3-methylimidazolium hexafluorophosphate (BMIM·PF<sub>6</sub>), also has been investigated electrochemically by AlNashef et al.,<sup>8</sup> as has the catalytic reduction of iodoethane and Freon 113 by electrogenerated nickel(I) salen in BMIM·BF<sub>4</sub>.<sup>9</sup>

In all of above-mentioned studies, the electroactive species were dissolved in the ionic liquid prior to oxidation or reduction to produce a chemically reactive entity. As an alternative to use of 1–10 mL volumes of ionic liquid containing a millimolar concentration of dissolved material, voltammetry of adhered microparticles/microdroplets is a useful technique for studying the redox properties of very small (microgram or less) quantities of species that are only sparingly soluble or kinetically slow to dissolve.<sup>10,11</sup> In these studies, arrays of microparticles/microdroplets can be mechanically adhered onto the working electrode surface. The modified electrode is then placed in contact with a conventional solvent/electrolyte combination or ionic liquid,<sup>11</sup> after which voltammetric measurements are undertaken. A detailed description of the experimental procedures, principles, and recent development of this method are available in reviews by Scholz<sup>10</sup> and Bond.<sup>11</sup>

In earlier publications,<sup>4</sup> we have demonstrated that a wide range of neutral redox active organometallic compounds adhered to the electrode surface are kinetically slow to dissolve in viscous ionic liquids. Intriguingly, oxidation or reduction to produce charged products facilitates their dissolution and enables reversible potentials to be obtained that are indistinguishable from that obtained from organometallic compounds dissolved in the ionic liquid after an extended period of sonication. In this study, we describe the use of this technique to generate dissolved

\* Corresponding author. E-mail address: alan.bond@sci.monash.edu.au.

**CHART 1: Structure of Organometallic Compounds Used in This Study** [ $L = \text{P}(\text{OPh})_3$ ,  $\text{P}-\text{P} = \text{Ph}_2\text{PCH}_2\text{PPh}_2$ , and  $\text{P}'-\text{P}' = \text{Ph}_2\text{PCH}_2\text{CH}_2\text{PPh}_2$ ]



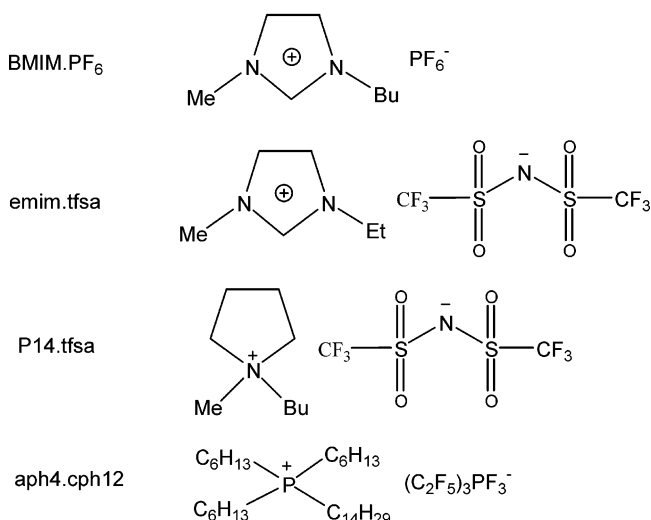
products that exhibit homogeneous first-order reactions that are coupled to the electron-transfer–dissolution process. The reason for restricting our quantitative studies to reactions involving first-order coupled homogeneous reaction is that the evaluation of the voltammetric response of this type of process is independent of the reactant or product concentrations, which are unknown under these initially adhered solid-state conditions. Two redox systems that have been well studied in organic solvent (electrolyte) media are now considered in ionic liquid media: the one-electron oxidation of *cis*-[ $\text{Mn}(\text{CN})(\text{CO})_2\{\text{P}(\text{OPh})_3\}(\text{DPM})$ ] ( $\text{DPM} = \text{Ph}_2\text{PCH}_2\text{PPh}_2$ ) (*cis*-Mn)<sup>12</sup> and *cis*-[ $\text{W}(\text{CO})_2(\text{DPE})_2$ ] ( $\text{DPE} = \text{Ph}_2\text{PCH}_2\text{CH}_2\text{PPh}_2$ ) (*cis*-W)<sup>11,13</sup> to their *cis*<sup>+</sup> forms followed by first-order isomerization to their *trans*<sup>+</sup> structures. The rate constants for the isomerization processes have been obtained in four hydrophobic ionic liquids that have widely varying physical and chemical properties: BMIM•PF<sub>6</sub>, (1-ethyl-3-methylimidazolium)bis[(trifluoromethyl)sulfonyl]amide (emim•tfsa), (*N*-butyl-*N*-methylpyrrolidinium)bis[(trifluoromethyl)sulfonyl]amide (P14•tfsa), and trihexyl(tetradecyl)phosphonium tris(pentafluoroethyl)trifluorophosphate (aph4•cph12).

## Experimental Section

**Chemicals.** Cobalticinium hexafluorophosphate, [ $\text{CoCp}_2$ ][PF<sub>6</sub>] (98%) was purchased and used as supplied by Strem Chemicals. *cis*-Mn and *cis*-W (see Chart 1) were synthesized, purified, and characterized according to the literature procedures.<sup>12,14,15</sup> Acetonitrile (HPLC grade, Merck) was used as received. Bu<sub>4</sub>NPF<sub>6</sub> was obtained from GFS and recrystallized twice according to the literature procedure.<sup>16</sup> The ionic liquids: BMIM•PF<sub>6</sub> (>97%, Sigma-Aldrich), emim•tfsa, and P14•tfsa (synthesized according to literature procedures<sup>17,18</sup>) and aph4•cph12 (Merck) were dried and purified before use over basic alumina for at least 24 h to minimize the presence of trace water and other contaminants. These four hydrophobic ionic liquids were chosen because they are easy to handle experimentally, allow the species of interest to be dissolved (after a significant period of sonication), have a range of physical and chemical properties, and have a wide potential window. The structures of BMIM•PF<sub>6</sub>, emim•tfsa, P14•tfsa, and aph4•cph12 are presented in Chart 2. Some physical properties of these ionic liquids are highlighted in the Table 1, as are the properties of acetonitrile (CH<sub>3</sub>CN), acetone, and dichloromethane (CH<sub>2</sub>Cl<sub>2</sub>), which represent typical organic solvents widely used in electrochemical studies and water.

**Instrumentation and Procedures.** Voltammetric, bulk electrolysis, and uncompensated resistance experiments were undertaken with a BAS 100B (Bioanalytical Systems) electrochemical workstation. A conventional three-electrode cell was employed, with 1 mm diameter glassy carbon (GC) or 25 or 10

**CHART 2: Structures of Ionic Liquids Used in This Study**



$\mu\text{m}$  diameter Pt microdisk electrodes as the working electrodes and Pt wire as the counter electrode. A Ag wire dipped in a tube containing ionic liquid, which was separated from the test solution by a glass frit, was used as the quasi-reference electrode. The potential of the quasi-reference electrode was calibrated against that of the IUPAC recommended [ $\text{CoCp}_2$ ]<sup>+0</sup> process using a 1 mM [ $\text{CoCp}_2$ ][PF<sub>6</sub>] solution ( $\text{CoCp}_2 = \text{cobaltocene}$ ) as an internal reference.<sup>19</sup>

The procedure for mechanical attachment of microcrystalline particles onto electrode surfaces has been described in detail elsewhere.<sup>10,11</sup> In brief, a few milligrams of solid compounds was placed on weighing paper. The working electrode was then pressed onto the paper substrate and rubbed over the solid so that some of the microcrystalline solid adhered to the electrode surface. This microparticle modified electrode was then directly placed in contact with ionic liquid. Prior to the attachment of solid, working electrodes were polished with a 0.05  $\mu\text{m}$  Al<sub>2</sub>O<sub>3</sub> (Buehler) slurry, washed successively with water and acetone, and finally dried with tissue paper.

The bulk electrolysis method was used to prepare [*trans*-W][PF<sub>6</sub>]. The working and auxiliary electrodes made from cylindrical platinum gauze were used. The reference electrode employed was a Ag/AgCl electrode (CH<sub>2</sub>Cl<sub>2</sub> saturated with LiCl), which was separated from the test solution by a salt bridge containing CH<sub>2</sub>Cl<sub>2</sub> (0.010 M Bu<sub>4</sub>NPF<sub>6</sub>). The working and the reference electrodes were placed in a glass cylinder (total volume  $\sim 12$  mL) filled with 10 mL of a saturated CH<sub>2</sub>Cl<sub>2</sub> (0.010 M Bu<sub>4</sub>NPF<sub>6</sub>) solution of *cis*-W (ca. 1 mM). This glass cylinder, which contained a porous frit in its base, was placed in a larger cylindrical glass cell containing the auxiliary electrode and approximately 15 mL of CH<sub>2</sub>Cl<sub>2</sub> (0.010 M Bu<sub>4</sub>NPF<sub>6</sub>) to physically separate the working and auxiliary electrodes. Stirring bars were placed in both the inner and outer cylinders. During bulk electrolysis, the potential of the working electrode was held at 0.40 V vs Ag/AgCl (or 1.25 V vs [ $\text{CoCp}_2$ ]<sup>+0</sup>) and the solution was stirred vigorously. The electrolysis was stopped when the ratio of the average current during a time interval achieved a value of 1% of that obtained at the commencement of the experiment. The solvent was partially evaporated to give solid [*trans*-W][PF<sub>6</sub>], which was collected by filtration. The produced [*trans*-W][PF<sub>6</sub>] was dissolved in and recrystallized twice from CH<sub>2</sub>Cl<sub>2</sub> before use.

To prepare ionic liquid solutions containing a known concentration of *cis*-Mn, the ionic liquid containing the appropriate

TABLE 1: Comparison of Some Physical Properties of Ionic Liquids, Organic Solvents and Water<sup>16</sup>

ionic liquid or neutral solvent	viscosity/ cP	density	conductivity/ mS cm <sup>-1</sup>	nominal molar ionic concentration <sup>a</sup> /M	dielectric constant or polarity
BMIM•PF <sub>6</sub> <sup>b</sup>	312 <sup>c</sup>	1.37 <sup>c</sup>	6.56 <sup>d</sup>	4.82	polarity is comparable to that of organic solvents, such as acetonitrile and alcohol. <sup>j</sup>
emim•tfsa <sup>e</sup>	35	1.520	9.6	3.89	
P14•tfsa <sup>f</sup>	85 <sup>g</sup>	1.41 <sup>h</sup>	2.2 <sup>g</sup>	3.34	
aph4•cph12 <sup>g,i</sup>	587.4	1.18	0.0809	1.27	
CH <sub>3</sub> CN	0.33 <sup>c</sup>	0.7766 <sup>k</sup>	7.58 <sup>l</sup>	n	37.5 <sup>g</sup>
CH <sub>2</sub> Cl <sub>2</sub>	0.39 <sup>c</sup>	1.3168 <sup>k</sup>	1.38 <sup>l</sup>	n	8.93 <sup>k</sup>
acetone	0.30 <sup>k</sup>	0.7844 <sup>k</sup>	5.52 <sup>l</sup>	n	20.7 <sup>k</sup>
H <sub>2</sub> O	0.89 <sup>k</sup>	0.9970 <sup>k</sup>	12.86 <sup>m</sup>	n	78.4 <sup>k</sup>

<sup>a</sup> Calculated using the equation: molar concentration = 1000 × density / molecular weight. <sup>b</sup> Data obtained from ref 1b. <sup>c</sup> Measured at 30 °C. <sup>d</sup> Measured at 60 °C. <sup>e</sup> Data obtained from ref 2b and were measured at 20 °C except for the value of density which was measured at 22 °C. <sup>f</sup> Data obtained from ref 18. <sup>g</sup> Measured at 20 °C. <sup>h</sup> Measured at 25 °C. <sup>i</sup> Data obtained from Merck. <sup>j</sup> Data obtained from ref 1a,f. <sup>k</sup> Measured at 35 °C. Data obtained from ref 16. <sup>l</sup> 0.1 M Bu<sub>4</sub>NClO<sub>4</sub> and measured at 22 °C. Data obtained from ref 28. <sup>m</sup> 0.1 M KCl and measured at 25 °C. Data obtained from ref 16. <sup>n</sup> Typically 0.1 to 1 M supporting electrolyte is present in electrochemical studies.

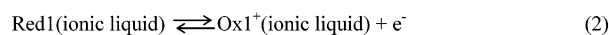
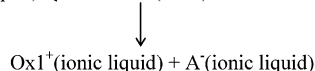
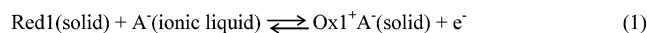
amount of solid *cis*-Mn was left in an ultrasonic cleaner (Unisonics Pty Ltd. Australia) and the solution was shaken from time to time to enhance the dissolution process. Typically, 1–2 h of sonication was required to completely dissolve the quantity of solid necessary to prepare mM or higher concentrations.

All experiments were conducted at ambient temperature of 20 ± 1 °C.

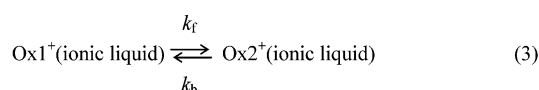
The commercial simulation package, DigiSim<sup>20</sup> was used to simulate cyclic voltammetric responses. Errors associated with the precision of reported first-order rate constant and diffusion coefficients are typically 10% and 5%, respectively.

## Theoretical Considerations

Voltammograms of microparticle arrays adhered to an electrode surface in contact with hydrophobic ionic liquids frequently exhibit classical behavior associated with those of the solution phase dissolved form.<sup>4</sup> The ability of voltammetric studies with adhered microparticles to be conveniently used in this manner to obtain the reversible formal potential of the solution phase form of the electron-transfer processes is attributed to the rapid dissolution of the electrogenerated form of solid and lack of reprecipitation of initially present form of the compound when present in the ionic liquid phase.<sup>4c</sup> Equations 1 and 2 describe the reactions that occur under these circumstances



where Red1 and Ox1<sup>+</sup> are the reduced and oxidized forms, respectively, and A<sup>-</sup> is the anionic component of ionic liquid. If this reaction scheme is extended via addition of a homogeneous chemical reaction (eq 3) to the electron-transfer process (eq 2), then the rate constants, (forward, *k<sub>f</sub>*, and backward, *k<sub>b</sub>*) or the equilibrium constant *K* = *k<sub>f</sub>* / *k<sub>b</sub>* may be measurable.



A major limitation in quantitative evaluation of the extended reaction scheme is that considerable uncertainty exists with several of the experimental parameters. For example, the distribution and sizes of the microparticles on the electrode surface as well as the details of the diffusion processes in the solid state and the kinetics of the dissolution processes are

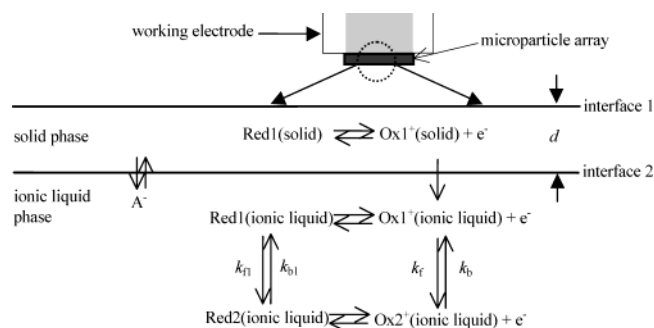


Figure 1. Schematic representation of the principal processes assumed to influence the voltammetric response when a microparticle modified electrode is placed in contact with an ionic liquid and when dissolved electrogenerated species Ox1<sup>+</sup>(ionic liquid) undergoes a square reaction scheme.

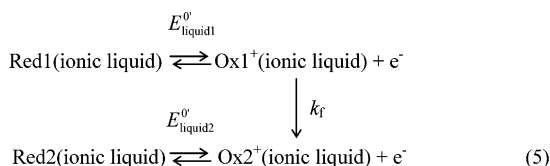
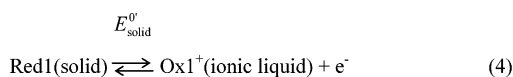
unknown. Consequently, the concentration of dissolved electrogenerated species in the ionic liquid phase, which subsequently undergoes a chemical reaction, is unlikely to be known. However, quantitative evaluation of the kinetics of a first-order chemical reaction is viable because the voltammetric characteristics of this family of reactions is independent of the concentration of electrochemically generated material.

Figure 1 provides a schematic diagram that illustrates the principal processes believed to be involved in the oxidation of microparticles of redox active species adhered to an electrode surface in contact with an ionic liquid<sup>4</sup> and when dissolved electrogenerated species Ox1<sup>+</sup>(ionic liquid) undergoes a square reaction scheme.<sup>7</sup> To model the voltammetry, the arrays of microparticle islands present are treated as the summation of individually functioning separated layers.<sup>4</sup>

The symbols Red1, Red2 (reduced form) and Ox1<sup>+</sup>, Ox2<sup>+</sup> (oxidized form) (see Figure 1) represent the general case. *k<sub>f</sub>*, *k<sub>f1</sub>* and *k<sub>b</sub>*, *k<sub>b1</sub>* in Figure 1 are the first-order rate constants of forward and backward chemical reactions, respectively, with the equilibrium constant of chemical reaction, *K*<sub>1</sub> and *K*<sub>2</sub> being equal to *k<sub>f</sub>* / *k<sub>b</sub>* and *k<sub>f1</sub>* / *k<sub>b1</sub>*, respectively. In the model employed, the rates of both dissolution of Red1(solid) and reprecipitation of Red1(solid) and Red2(solid), even if thermodynamically allowed, are assumed to be negligibly slow on the voltammetric time scale. The initially important processes that contribute to the voltammetry therefore are assumed to be the oxidation of Red1(solid) to Ox1<sup>+</sup>(solid), which is accompanied by charge neutralization involving the insertion of A<sup>-</sup> into the solid and the dissolution of [Ox1][A](solid). The equilibrium relationships between the dissolved (Ox1<sup>+</sup>(ionic liquid) and A<sup>-</sup>(ionic liquid)) species and [Ox1][A](solid) at the particle/ionic liquid interface are assumed to be established on the voltammetric time scale.



Moreover, for the isomeric reactions considered in this paper, only  $k_f$  is believed to be significant on the voltammetric time scale.<sup>11,12,13</sup> Thus, the processes to be simulated are



In this reaction scheme,  $E_{\text{solid}}^0$ ,  $E_{\text{liquid1}}^0$ , and  $E_{\text{liquid2}}^0$  are the formal potentials of processes described by eqs 4 and 5 [ECE (first-order C) reaction scheme].

The process in eq 4 is akin to that found in classical stripping voltammetry,<sup>7</sup> and the mechanism described in eqs 4 and 5 may be simulated using concepts introduced previously.<sup>4a,c</sup> In brief, it is assumed for each island of solid adhered to the electrode surface that both the solid and solution phase  $\text{Ox1}^+/\text{Red1}$  and  $\text{Ox2}^+/\text{Red2}$  processes occur at interface 2 shown in Figure 1 and exhibit reversible one-electron-transfer reactions so that activities of all relevant species at the particle/ionic liquid interface are governed by the Nernst equation. Thus, the voltammetric response detected is the sum of that associated with each island of a solid. Furthermore, the modeling assumes the absence of reactions between any oxidized and reduced species and the theoretical analysis does not take into account any change of solid thickness arising from the dissolution process.<sup>4a</sup> The theoretical treatment applied to each island of solid is similar to that used to describe the behavior of redox active layer modified electrodes.<sup>7</sup> This kind of model also was adopted in a numerical simulation of a related, but simpler process.<sup>21</sup> However, the activities of  $\text{Red1(solid)}$  and  $\text{Ox1(solid)}$  are not known, and the assumption that these activities are proportional to their mole fraction is only used because of its inherent simplicity.

As a consequence of employing the model summarized above, mass transport inside a binary solid phase is assumed to be fully diffusion mediated, noting in any case that any hopping type electron-transfer process within the solid may be treated as an overall diffusion problem having an apparent diffusion coefficient.<sup>22,23</sup> A one-dimensional linear diffusion equation is applied to this model. In a previous paper,<sup>4c</sup> we demonstrated that an asymmetrical voltammogram is expected if the mass of solid particle on the electrode surface is not sufficient to provide a continuous supply of dissolved material. In the present study, there is always sufficient amount of electroactive material adhered on the electrode surface to prevent this from happening. The situation encountered therefore corresponds to a theoretical case where the thickness of the adhered solid islands,  $d$ , is large enough for the semi-infinite diffusion to be appropriate for the solid state species. Consequently, semi-infinite diffusion is applicable to all species involved in the reactions described by eqs 4 and 5. Under such a circumstance, the commercially available electrochemical simulation package, DigiSim<sup>20</sup> may be very conveniently used to model the reaction scheme described by eqs 4 and 5, using principles adapted from ref 21.

To demonstrate that the voltammetry of adhered microparticles can be used to obtain the rate constants for first-order coupled homogeneous reaction, simulations of mechanisms of both adhered solid and dissolved species based on the mechanisms described in eqs 4 and 5 (adhered solid state) and eq 5

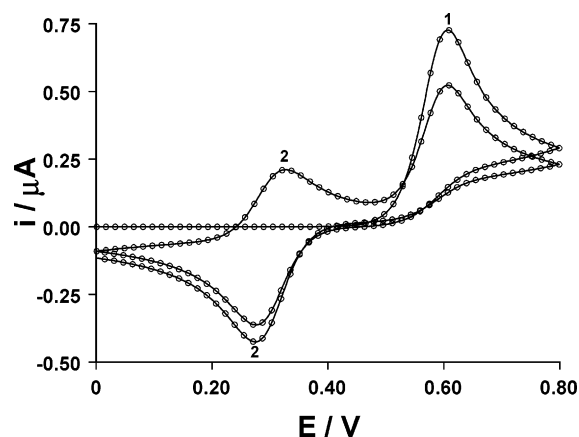


**Figure 2.** Normalized simulated voltammograms of adhered solid (—) and dissolved state (○) species which undergo an ECE (first-order C) reaction. Parameters used in the simulation are defined in the text. The peak current of simulated voltammogram obtained from the dissolved state has been normalized to that of the solid state form to demonstrate the shape and peak potential equivalence. Numbers 1 and 2 in this and the following figures designate the first and second cycle of potential, respectively.

(fully dissolved state) were undertaken. The simulated results employed the arbitrary parameters of  $c_{\text{solid}}^* = 1 \text{ M}$ ,  $D_{\text{solid}} = 1 \times 10^{-11} \text{ cm}^2 \text{ s}^{-1}$ ,  $D_{\text{solution}} = 1 \times 10^{-8} \text{ cm}^2 \text{ s}^{-1}$  (typical for a viscous ionic liquid), and radius of electrode = 0.05 cm, where  $c_{\text{solid}}^*$ ,  $D_{\text{solid}}$ , and  $D_{\text{solution}}$  are the bulk concentration of  $\text{Red1(solid)}$ , diffusion coefficient of  $\text{Red1(solid)}$ , and diffusion coefficient of all solution phase species, respectively;  $E_{\text{solid}}^0 = 0.50 \text{ V}$ ,  $E_{\text{liquid1}}^0 = 0.65 \text{ V}$ ,  $E_{\text{liquid2}}^0 = 0.30 \text{ V}$ ,  $k_f = 50 \text{ s}^{-1}$ ,  $v = 0.1 \text{ V s}^{-1}$  and all electron-transfer processes are assumed to be reversible. The value of 0.50 V used for  $E_{\text{solid}}^0$ , being less positive than 0.65 V, ensures that the simulated voltammogram obtained for the adhered microparticles when the product dissolves is identical to that of fully dissolved species when only the reactions described by eqs 4 and 5 in the absence of coupled homogeneous process and the corresponding extra electron-transfer reaction are considered.<sup>4a,c</sup> The normalized simulated results obtained under these conditions are presented in Figure 2 and confirm that voltammograms obtained from either the adhered or the dissolved state are equivalent.

Voltammetric characteristics of adhered solid, except the magnitude of peak current, when simulated on the basis of mechanism described in eqs 4 and 5 are independent of  $c_{\text{solid}}^*$  and  $D_{\text{solid}}$ , which is a highly valued property because these terms are unlikely to be known. Moreover, although the simulated results in Figure 2 are obtained using equal diffusion coefficients for all dissolved species and assume that all electron-transfer reactions are reversible, the equivalence between the normalized simulated voltammogram of adhered solid and dissolved material also applies in the absence of these restrictions (results not shown) and are widely applicable to other forms of electrochemical process with coupled first-order chemical reactions (results not shown).

## Results and Discussion

**Voltammetry of *cis*-Mn in Ionic Liquids.** The oxidation of *cis*-Mn follows an ECE (first-order C) mechanism involving isomerization of *cis*- $\text{Mn}^+$  to *trans*- $\text{Mn}^+$ , which is in turn reduced to *trans*-Mn.<sup>12</sup> First-order *cis* $^+$   $\rightarrow$  *trans* $^+$  isomerization reactions of this type are common.<sup>11,13,24</sup> Importantly, *cis*-Mn can be dissolved in ionic liquids after extensive sonication, so rate

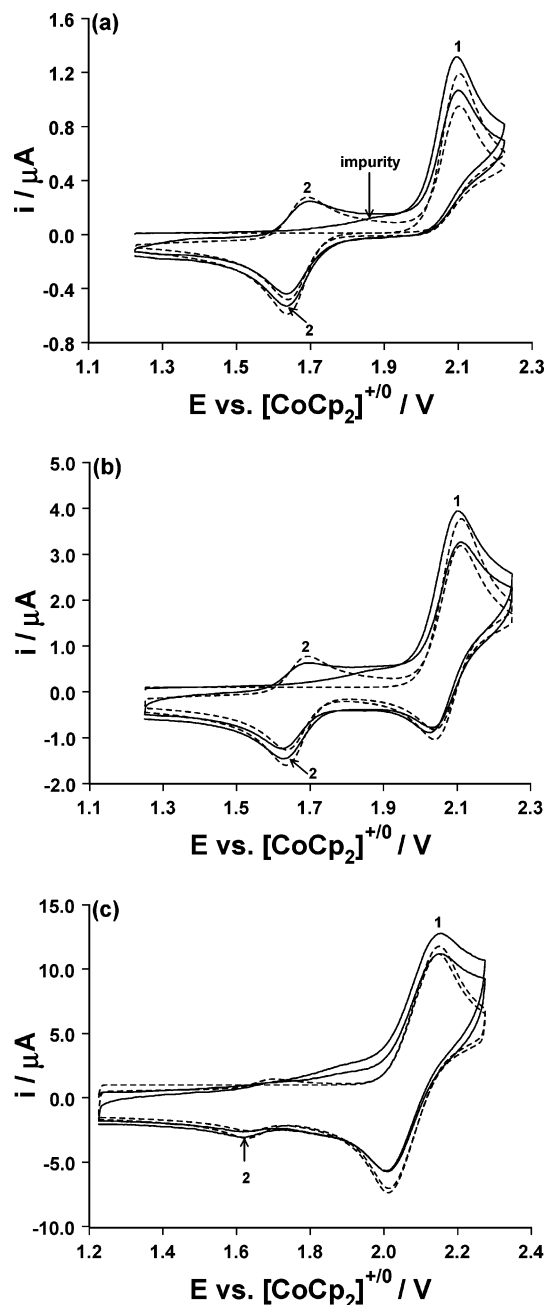


**Figure 3.** Cyclic voltammograms showing a comparison of experimental (—) results for the oxidation of 5.0 mM *cis*-Mn in the ionic liquid emim·tfsa at a 1 mm diameter GC electrode and normalized simulated (---) results obtained as a range of scan rates according to the mechanism described in eq 6, with  $k_f = 4 \text{ s}^{-1}$ ,  $E_{\text{liquid1}}^{0'} = 2.075 \text{ V}$ , and  $E_{\text{liquid2}}^{0'} = 1.665 \text{ V}$  (vs  $[\text{CoCp}_2]^{+/0}$ ). Scan rates are 0.1 (a), 1.0 (b), and 10.0 (c)  $\text{V s}^{-1}$ .

constants related to ionic liquid media may be calculated by conventional voltammetric techniques and data then compared against that found from the adhered solid form of voltammetry to confirm the equivalence of the two approaches. In the dissolved state, the ECE reaction scheme is summarized by eq 6.

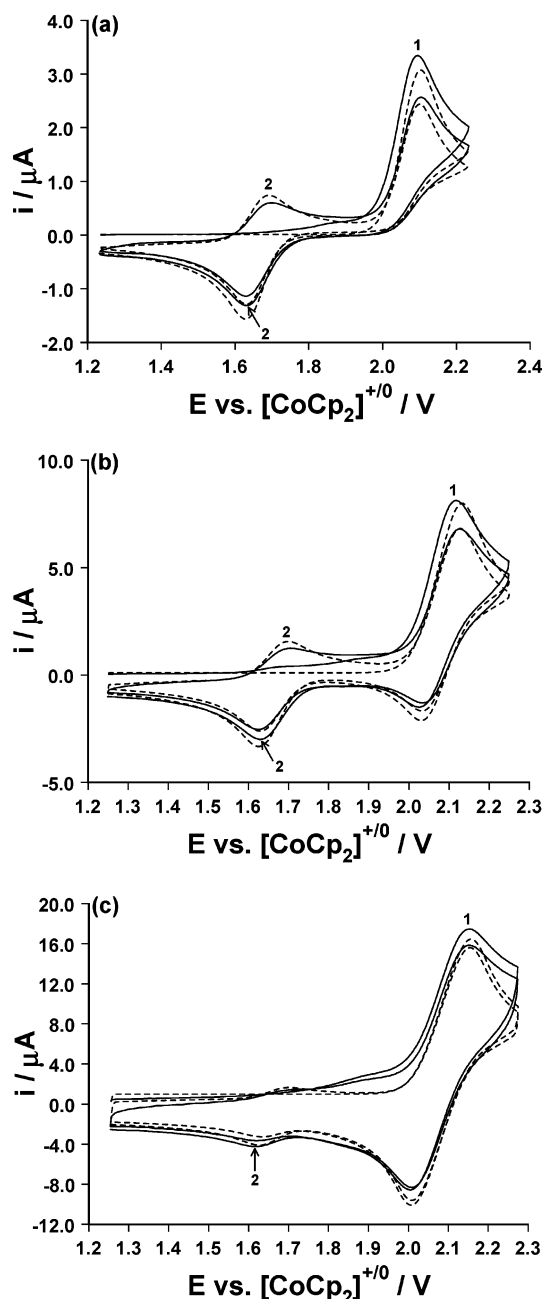
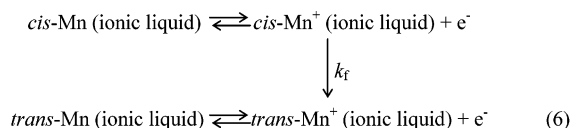


**Figure 4.** Cyclic voltammograms showing a comparison of experimental (—) results for the oxidation of *cis*-Mn microparticles mechanically adhered to a 1 mm diameter GC electrode surface prior to being placed in contact with emim·tfsa and normalized simulated (---) results obtained according to the mechanism described in eq 8, with  $k_f = 4 \text{ s}^{-1}$ ,  $E_{\text{liquid1}}^{0'} = 2.075 \text{ V}$ , and  $E_{\text{liquid2}}^{0'} = 1.665 \text{ V}$  (vs  $[\text{CoCp}_2]^{+/0}$ ). Scan rates are 0.1 (a), 1.0 (b), and 10.0 (c)  $\text{V s}^{-1}$ .

**Voltammetry of *cis*-Mn Dissolved in emim·tfsa.** The cyclic voltammetric oxidation of *cis*-Mn (5.0 mM) dissolved in emim·tfsa was investigated using a 1 mm diameter GC electrode and a range of scan rates.

Figure 3 reveals that excellent agreement between experimental and normalized simulated (according to the mechanism shown in eq 6) results are obtained at all scan rates examined with  $k_f = 4 \text{ s}^{-1}$  and other parameters contained in the caption to Figure 3. A small peak of unknown origin is present in Figure 3, but not included in the simulation. This peak was not observed in emim·tfsa in the absence of *cis*-Mn and also was not observed when *cis*-Mn was dissolved in acetonitrile. Furthermore, its peak

**TABLE 2: Summary of Thermodynamic, Kinetic, and Other Parameters Derived from Voltammetric Oxidation of *cis*-Mn in Ionic Liquids<sup>a</sup> and Conventional Solvents<sup>b</sup>**

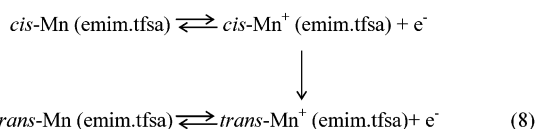
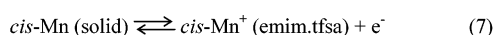
solvent	dissolved state					adhered solid state			
	$E_{\text{liquid1}}^{0'}/V^c$	$E_{\text{liquid2}}^{0'}/V^c$	$k_f/s^{-1}$	$10^{-7}K_1/K_2^d$	$10^8D/cm^2 s^{-1}$	$E_{\text{liquid1}}^{0'}/V^c$	$E_{\text{liquid2}}^{0'}/V^c$	$k_f/s^{-1}$	$10^{-7}K_1/K_2^d$
BMIM.PF <sub>6</sub>	2.085	1.675	4	1.13	1.0	2.085	1.675	4	1.13
emim.tfsa	2.075	1.665	4	1.13	10.0	2.075	1.665	4	1.13
P14.tfsa	2.050	1.640	4	1.13	3.9	2.050	1.640	4	1.13
aph4.cph12	1.990	1.530	40 <sup>e</sup>	8.18	0.72	1.990	1.530	40	8.18
CH <sub>3</sub> CN <sup>g</sup>	2.035	1.540	38 <sup>f</sup>	32.7	720	not applicable			
CH <sub>2</sub> Cl <sub>2</sub> <sup>f</sup>	2.040	1.545	38 <sup>f</sup>	32.7	600				

<sup>a</sup> This study. <sup>b</sup> Values reported at  $20 \pm 2$  °C in ref 12a in the presence of 0.1 M Bu<sub>4</sub>NPF<sub>6</sub> as the supporting electrolyte. A 25 μm diameter Pt microdisk electrode was utilized. We find  $k_f$  value obtained with a 100 μm diameter Pt microdisk electrode to be  $40 \pm 4$  s<sup>-1</sup> and independent of electrolyte concentration (see text) in CH<sub>3</sub>CN. <sup>c</sup> Vs [CoCp<sub>2</sub>]<sup>+0</sup>. <sup>d</sup> Calculated from the relationship  $K_1/K_2 = \exp[(F/RT)(E_{\text{liquid1}}^{0'} - E_{\text{liquid2}}^{0'})]$  that can be derived from the reaction scheme shown in Figure 1. <sup>e</sup> Measured voltammetrically using a 25 μm diameter Pt microdisk working electrode instead of a 1 mm diameter GC electrode to minimize uncompensated resistance effect. <sup>f</sup> Potential (versus Fc<sup>0/+</sup> in ref 12a) converted to the values versus [CoCp<sub>2</sub>]<sup>+0</sup> process using the known difference between the formal potential of these processes.<sup>29</sup>

height diminished on purification of the ionic liquid with basic alumina. This peak most likely arises from the presence of reaction between a trace impurity such as water or halide in emim.tfsa, but rate constant data are not affected by the presence of this impurity ( $k_f$  values are independent of *cis*-Mn concentration).

Both electron-transfer processes in the  $\bar{E}CE$  scheme are assumed to be fully reversible whereas the chemical reaction coupled to the electron-transfer process is assumed to be fully irreversible. Uncompensated ionic liquid resistance ( $R_u$ ) and background charging current are included in the simulation. Although, ionic liquids contain a significant ionic concentration, the mobility of ions is often poor due to their high viscosity, so that  $R_u$  values are fairly large. Typically, uncompensated resistance values of 3000 Ω (emim.tfsa), 5000 Ω (BMIM.PF<sub>6</sub>), 6000 Ω (P14.tfsa), and 70000 Ω (aph4.cph12) were found experimentally in studies in the dissolved state when a 1 mm GC electrode was used as working electrode and the separation between the working and reference electrode tip was 2 mm.  $R_u$  is in the range found for CH<sub>2</sub>Cl<sub>2</sub> (0.1 M Bu<sub>4</sub>NPF<sub>6</sub>) except the case of aph4.cph12, which has a much higher value. A capacitance value of 15 μF cm<sup>-2</sup> was typically used in simulations associated with the GC working electrode. Diffusion coefficients of all species were assumed to be equal, and the actual value acts solely as a scaling factor. Consequently, values of real current obtained experimentally enable the value of  $D$  to be established, but simulated data could be normalized to experimental data for the purpose of calculation of  $k_f$ .

**Voltammetry of Adhered *cis*-Mn Microparticles in Contact with emim.tfsa.** Voltammograms can be recorded easily when an electrode modified with microparticles of neutral *cis*-Mn is placed in contact with emim.tfsa, because unlike the presumed situation with cationic solid *cis*-Mn<sup>+</sup> or *trans*-Mn<sup>+</sup>, the rate of dissolution of adhered nonoxidized solid is extremely slow. Major processes involved when commencing with a *cis*-Mn modified electrode are summarized in eqs 7 and 8:

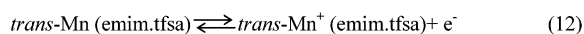
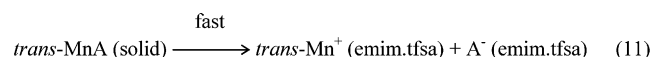
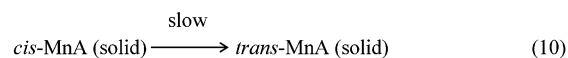
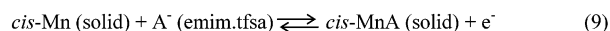


A comparison of experimental and simulated voltammograms are shown in Figure 4, with parameters employed in the simulation being summarized in the caption of the figure.  $R_u$

values obtained under these conditions are slightly higher than for studies in the dissolved state because of contribution, from adhered nonconducting *cis*-Mn microparticles. Thermodynamic ( $E_{\text{liquid1}}^{0'}$  and  $E_{\text{liquid2}}^{0'}$ ) and kinetic ( $k_f$ ) parameters obtained via use of simulation are indistinguishable within experimental error to those found when *cis*-Mn is studied in the dissolved state, implying that use of very small quantities of adhered solid is an extremely attractive method for obtaining these parameters.

Significantly higher concentrations of dissolved oxidized species are generated on the seconds time scale when the adhered solid method is employed (compare Faradaic peak current heights in Figures 3 and 4). Consequently, the relative influence from trace contaminants such as water or halides are minimized.

In principle, reaction schemes (such as the one shown in eqs 9–12) rather than the one summarized in eqs 7 and 8 could apply.



However, if this is the case, the equivalence between the voltammograms of dissolved form and adhered solid microparticle would not be expected, because a *cis*-MnA (solid) to *trans*-MnA (solid) transformation (eq 10) via a twist mechanism is predicted to be slower in the solid phase than is the case in the solution phase.<sup>12a,25</sup> Consequently, only electron-transfer reaction (eq 9) is assumed to be significant in these ionic liquid studies on the voltammetric time scale.

**Data Obtained in Other Ionic Liquids and Organic Solvents.** Formal reversible potentials,  $K_1/K_2$  ratios and  $k_f$  data obtained from voltammetric studies utilizing solid microparticle and dissolved form in four ionic liquids are summarized in Table 2 as are data obtained when *cis*-Mn is dissolved in common organic solvent such as CH<sub>3</sub>CN and CH<sub>2</sub>Cl<sub>2</sub> (0.1 M Bu<sub>4</sub>NPF<sub>6</sub>).<sup>12a</sup> Data obtained in ionic liquids are independent of whether microparticles of adhered solid or dissolved material are employed. The formal potentials obtained in the ionic liquids are not significantly different from those obtained in the conventional organic solvent (electrolyte) media, although the

values of the equilibrium constant ratios  $K_1/K_2$  are somewhat lower in the ionic liquid case. However, although the first-order isomerization rate constant value of  $40 \text{ s}^{-1}$  in aph4·cph12 is comparable to the value of  $38 \text{ s}^{-1}$  in conventional organic solvents (electrolyte) media, the  $k_f$  values in the other ionic liquids of  $4 \text{ s}^{-1}$  are an order of magnitude smaller.

Unlike the case in systems studied by Hapiot et al.,<sup>6</sup> data obtained in this study for the first-order  $cis^+ \rightarrow trans^+$  isomerization reaction clearly depend on the identity of the ionic liquid. No obvious correlation of  $k_f$  with the physical parameters given in Table 1 is evident. Diffusion coefficients obtained from the comparison of absolute current values found in the experimental and simulated results are also given in Table 2, but again show no simple correlation with  $k_f$  values. (Ideally, the diffusion coefficient is inverse proportional to the viscosity of the solvent according to Stokes–Einstein law.<sup>26</sup>) Because  $k_f$  values obtained also were found to be essentially independent of concentration of the supporting electrolyte,  $Bu_4NPF_6$ , over the range 10 mM to 1 M, the ionic liquid identity dependence is unlikely to simply reflect the effect of ionic strength. The simple formation of ion pairs also probably cannot explain the results. For example, even though ion pair formation in the low dielectric constant  $CH_2Cl_2$  is significantly higher than in the more polar  $CH_3CN$  media, similar  $k_f$  values apply to both media, as expected for a twist mechanism. As the viscosity of  $BMIM \cdot PF_6$  and aph4·cph12 are comparable, the order of magnitude difference in the measured  $k_f$  value is not solely attributable to the influence of viscosity. The possibility of significant influence of trace impurities in some ionic liquids also is considered unlikely as  $k_f$  values are confirmed to be first order via the independence of the concentration of  $cis$ -Mn. The tentative conclusion is therefore reached that the value of  $k_f$  contains contributions from a complex combination of physical and chemical properties with the identity and property of the cation and anion involving in the ionic liquid probably having a significant effect. As revealed by examination of Chart 2, four different cations and three different anions of often significantly different structure have been used in this study. Extensive further studies will be needed to ascertain the origin of the dependence of  $k_f$  on the identity of the ionic liquid.

**Voltammetry of *cis*-W in Ionic Liquids.** In view of finding that the value of  $k_f$  appear to be a function of the identity of the ionic liquid in the case of isomerization of  $cis$ -Mn<sup>+</sup> to  $trans$ -Mn<sup>+</sup>, a second system was studied to confirm the generality of this result. In this case, the  $cis$ -W<sup>+</sup>  $\rightarrow$   $trans$ -W<sup>+</sup> isomerization step has been reported to have a value of  $44.5 \text{ s}^{-1}$  in acetone.<sup>13c</sup> However, in this case,  $cis$ -W is only sparingly soluble in the ionic liquids employed so that quantitative rate constant data can be obtained in the ionic liquid media only by using the adhered microparticle technique.

**Voltammetry of *cis*-W Dissolved in Ionic Liquids.** The solubility of  $cis$ -W in the ionic liquids employed in the present studies is very low. Thus, the background charging current dominates even when slow scan rates are employed with a saturated solution of  $cis$ -W (e.g., see Figure 5a for the  $BMIM \cdot PF_6$  case). Use of the faster scan rates required to calculate  $k_f$  is therefore not possible as the Faradaic to charging current ratio becomes too unfavorable. Based in Figure 6a, values of  $E_{liquid1}^{0'} = 1.12 \text{ V}$  and  $E_{liquid2}^{0'} = 0.75 \text{ V vs [CoCp}_2]^{+/0}$  and  $k_f > 10 \text{ s}^{-1}$  were obtained by comparing the experimental (Figure 5a) and the simulated voltammograms. However,  $[trans\text{-W}][PF_6]$  could be prepared via bulk electrolysis of  $cis$ -W and exhibits a much higher solubility (millimolar level). Importantly, it was found that this oxidized trans isomer dissolves rapidly in the ionic

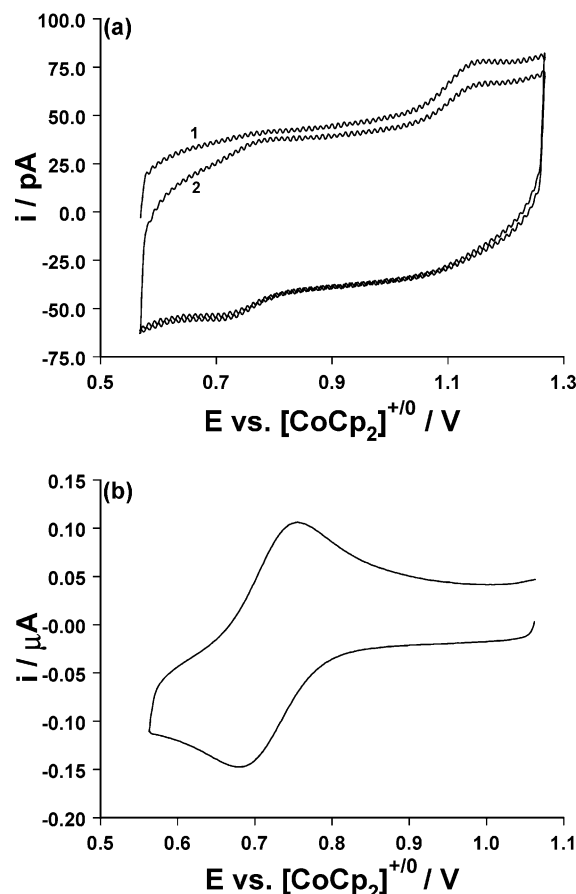


**Figure 5.** Cyclic voltammograms obtained at a scan rate of  $0.5 \text{ V s}^{-1}$  in  $BMIM \cdot PF_6$  for (a) the oxidation of dissolved  $cis$ -W (saturated solution) obtained at a  $25 \mu\text{m}$  diameter Pt microdisk electrode and (b) the reduction of  $1.0 \text{ mM } [trans\text{-W}][PF_6]$  solution at a  $1 \text{ mm}$  diameter GC electrode.

liquid, so that sonication was not required to prepare a  $1 \text{ mM}$   $BMIM \cdot PF_6$  solution of  $[trans\text{-W}][PF_6]$  used to obtain the Figure 5b voltammogram. The formal reversible potential of  $0.749 \text{ V vs [CoCp}_2]^{+/0}$  for  $E_{liquid2}^{0'}$  obtained from this experiment is in excellent agreement with the value of  $0.75 \text{ V vs [CoCp}_2]^{+/0}$  obtained from experiments with saturated  $cis$ -W. This result confirms that the  $cis$ -W<sup>+</sup> to  $trans$ -W<sup>+</sup> transformation takes place on the voltammetric time scale used in Figure 5a and supports the applicability of the reaction scheme (Figure 1), which requires the kinetics of dissolution of oxidized species should be much faster than is the case with the reduced form.

**Voltammetry of Adhered *cis*-W Microparticles in Contact with Ionic Liquids.** In contrast to the case where the low concentration of saturated solutions of dissolved  $cis$ -W limit the scan rate that can be used, well-defined voltammograms for the  $cis$ -W oxidation process can be easily obtained by the adhered microparticles method over the wide scan rate range required to calculate  $k_f$ . Typical results obtained for voltammetric oxidation of  $cis$ -W at a  $25 \mu\text{m}$  diameter Pt microdisk electrode in the ionic liquid  $emim \cdot tfsa$  are shown in Figure 6. Because the value of  $k_f$  for the  $cis$ -W<sup>+</sup>  $\rightarrow$   $trans$ -W<sup>+</sup> process is significantly higher than for the  $cis$ -Mn system, faster scan rates have to be used to evaluate  $k_f$ . This requirement leads to an enhanced uncompensated resistance effect. Therefore, for studies on the  $cis$ -W system in  $emim \cdot tfsa$  (and  $BMIM \cdot PF_6$  and  $P14 \cdot tfsa$ ), a  $25 \mu\text{m}$  diameter Pt microdisk electrode rather than GC macrodisc electrode was employed to minimize the influence of  $iR_u$  drop. An even smaller ( $10 \mu\text{m}$ ) diameter Pt microdisk



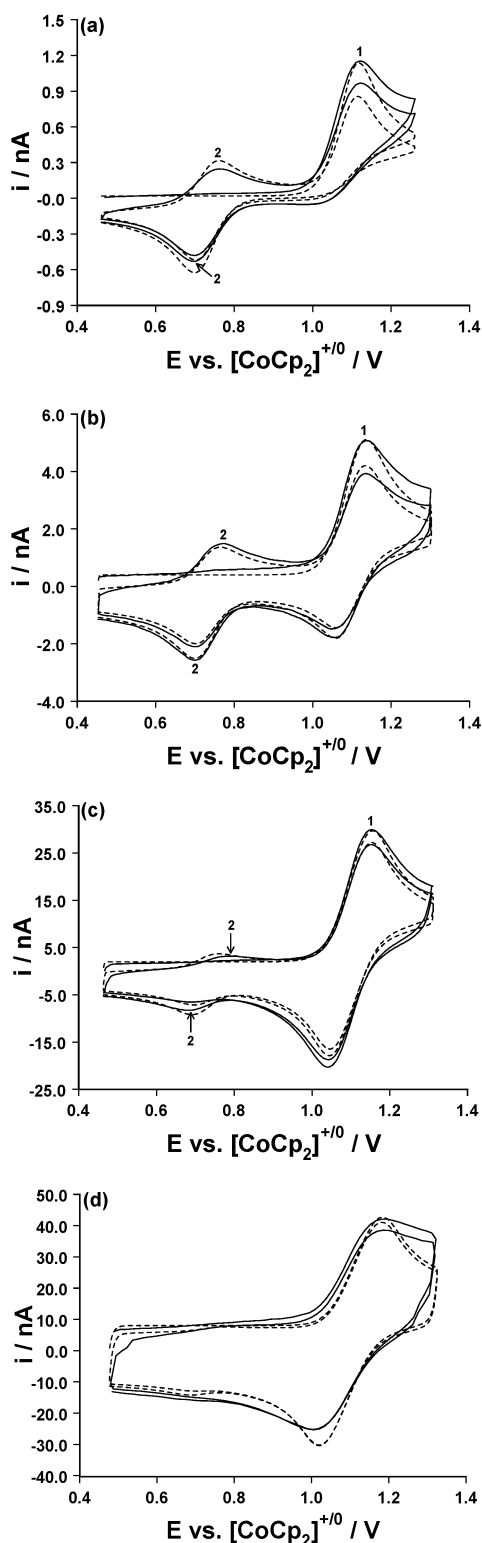


**Figure 6.** Cyclic voltammograms showing a comparison of experimental (—) results for the oxidation of *cis*-W microparticles mechanically adhered to a 25  $\mu\text{m}$  diameter Pt microdisk electrode surface prior to being placed in contact with emim $\cdot$ tfsa and normalized simulated results (---) obtained according to the mechanism described in eq 14, with  $k_f = 30 \text{ s}^{-1}$ ,  $E_{\text{liquid1}}^{0'} = 1.096 \text{ V}$  and  $E_{\text{liquid2}}^{0'} = 0.726 \text{ V}$  (vs  $[\text{CoCp}_2]^{+/0}$ ). Scan rates are 0.5 (a), 10 (b), 50 (c), and 200 (d)  $\text{V s}^{-1}$ .

electrode was employed in the very much higher resistance aph4 $\cdot$ cph12 ionic liquid. Appropriate values of  $R_u$  and double capacitance were employed in simulation at Pt microdisk

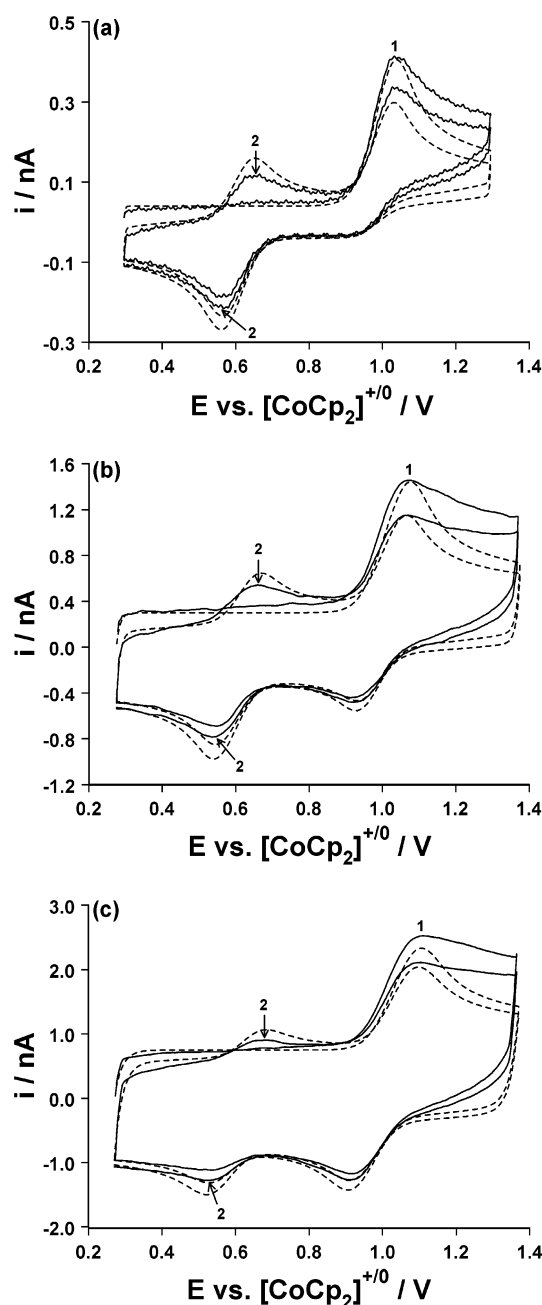
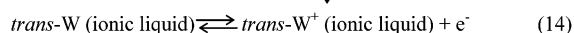
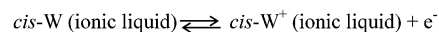
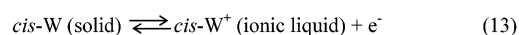


**Figure 7.** Cyclic voltammograms showing a comparison of experimental (—) results for the oxidation of *cis*-W microparticles which were mechanically adhered onto a 10  $\mu\text{m}$  diameter Pt microdisk electrode surface prior to being placed in contact with aph4 $\cdot$ cph12 and simulated results (---) obtained according to the mechanism described in eq 14, with  $k_f = 60 \text{ s}^{-1}$ ,  $E_{\text{liquid1}}^{0'} = 0.990 \text{ V}$ , and  $E_{\text{liquid2}}^{0'} = 0.610 \text{ V}$  (vs  $[\text{CoCp}_2]^{+/0}$ ). Scan rates are 0.5 (a), 20 (b), and 50 (c)  $\text{V s}^{-1}$ .

electrodes. The reaction scheme assumed to apply is summarized in eqs 13 and 14:



Voltammograms obtained with a *cis*-W microparticle array adhered to a 10  $\mu\text{m}$  diameter Pt microdisk electrode in contact with aph4 $\cdot$ cph12 are shown in Figure 7.



**TABLE 3: Summary of Thermodynamic and Kinetic Parameters Derived from Voltammetric Measurements When *cis*-W Is Mechanically Adhered to a Pt Microdisk Electrode Prior to Being Placed in Contact with Ionic Liquids<sup>a</sup> or Dissolved in Acetone**

solvent and electrolyte	$E_{\text{liquid1}}^{0'}/\text{V}^b$	$E_{\text{liquid2}}^{0'}/\text{V}^b$	$k_f/\text{s}^{-1}$	$10^{-6}K_1/K_2$
BMIM·PF <sub>6</sub> <sup>c</sup>	1.120	0.748	11	2.51
emim·tfsa <sup>c</sup>	1.096	0.726	30	2.32
P14·tfsa <sup>c</sup>	1.065	0.720	20	3.44
aph4·cph12 <sup>d</sup>	0.990	0.610	60	3.44
acetone	1.025 <sup>e</sup>	0.665 <sup>e</sup>	44.5 <sup>f</sup>	1.56

<sup>a</sup> This study. <sup>b</sup> Vs [CoCp<sub>2</sub>]<sup>+0</sup>. <sup>c</sup> Diameter of Pt working electrode = 25  $\mu\text{m}$ . <sup>d</sup> Diameter of Pt working electrode = 10  $\mu\text{m}$ . <sup>e</sup> Measured at 20 °C in the presence of 0.1 M Bu<sub>4</sub>NPF<sub>6</sub>. <sup>f</sup> Value reported at 25 °C in ref 13c in the presence of 0.1 M Et<sub>4</sub>NClO<sub>4</sub> as the supporting electrolyte.

A summary of thermodynamic and kinetic parameters obtained from voltammetric studies is contained in Table 3. For the *cis*-W system, the formal potentials and the difference in the formal potential of two redox processes are comparable (similar  $K_1/K_2$  value) in all ionic liquids examined and also comparable to those obtained in the acetone (electrolyte) media. Trends in  $k_f$  values are the same as for the *cis*-Mn<sup>+</sup> → *trans*-Mn<sup>+</sup> process. Thus, the  $k_f$  value of 60 s<sup>-1</sup> in aph4·cph12 is also similar to the value of 40 s<sup>-1</sup> reported in acetone (0.1 M Et<sub>4</sub>NClO<sub>4</sub>),<sup>13c</sup> but faster than found in the other ionic liquids examined. However, for the *cis*-W system,  $k_f$  is only a factor of 2–5 faster in aph4·cph12 than in the other ionic liquids rather than the factor of 10 faster found for the *cis*-Mn system. Nevertheless, the results obtained with *cis*-W imply again that data depend on the identity of the ionic liquid in a manner related to that found with *cis*-Mn.

## Conclusions

Commonly, neutral organometallic compounds have been found to be sparingly soluble or kinetically slow to dissolve in ionic liquids. In contrast, charged products formed by electrolysis can be far more soluble and dissolve very rapidly in ionic liquids. Experimental and theoretical studies suggest that under these circumstances voltammetric measurements with organometallic microparticles adhered to an electrode in contact with ionic liquids may facilitate the quantitative measurements of first-order homogeneous process coupled to the electron-transfer process. Electrochemical studies on  $\text{EC}_\text{E}$  (first-order C) model systems confirm in the case of the *cis*-Mn<sup>+</sup> → *trans*-Mn<sup>+</sup> process that experimentally indistinguishable data are obtained when the reaction is studied using adhered microparticles of *cis*-Mn or *cis*-Mn dissolved in ionic liquids after an extensive period of sonication. In the case of the *cis*-W system that gives rise to a *cis*-W<sup>+</sup> → *trans*-W<sup>+</sup> isomerization reaction after oxidation, only the adhered microparticle method could be used as *cis*-W is only sparingly soluble in the ionic liquids employed. However, studies on rapidly dissolved *trans*-W<sup>+</sup> confirm the  $\text{EC}_\text{E}$  mechanism is applicable in ionic liquids as is the case in organic solvents. Studies with the *cis*-W system also confirmed that the inherently simple adhered microparticle method facilitates the measurement of first-order rate constants.

$k_f$  values obtained from both *cis*-Mn and *cis*-W  $\text{EC}_\text{E}$  processes were found to be a function of ionic liquid identity. In the case of aph4·cph12,  $k_f$  is similar to the value found in organic solvent (electrolyte) media, but significantly faster than in the ionic liquids, BMIM·PF<sub>6</sub>, emim·tfsa and P14·tfsa. No simple correlation of  $k_f$  values for these first-order isomerization reactions

with the physical or chemical properties of ionic liquids has been elucidated. However, it is noteworthy that the dependence on ionic liquid identity differs from the case considered by Hapiot et al.,<sup>6</sup> who found the first-order rate constant for a durene cation radical → neutral radical process is not significantly influenced by the use of ionic liquids as an alternative solvent to organic (electrolyte) media. In the systems we have studied, solvent independent kinetics are observed for the twist isomerization mechanism that occur in conventional organic solvent/electrolyte media.<sup>11,13</sup> A medium dependence in ionic liquids could arise if the isomerization mechanism changes to one involving bond dissociation-bond formation.<sup>27</sup> Clearly, further extensive studies are needed before generalizations on the role of ionic liquids on rate constants of first-order processes can be reached.

**Acknowledgment.** We acknowledge the Australian Research Council and the Monash University Research Fund for financial support of this project. Professor Douglas MacFarlane and his research group (School of Chemistry, Monash University) are also thanked for their generous provision of the ionic liquids (emim·tfsa and P14·tfsa). Prof. Neil Connelly (School of Chemistry, University of Bristol) is acknowledged for his generous donation of *cis*-[Mn(CN)(CO)<sub>2</sub>{P(OPh)<sub>3</sub>}(DPM)] as is Merck for a gift of aph4·cph12 and provision of the data associated with its physical properties.

## References and Notes

- (1) (a) *Ionic Liquids in Synthesis*; Wasserscheid, P., Welton, T. Ed.; Wiley-VCH: Weinheim, 2002. (b) Dupont, J.; de Souza, R. F.; Suarez, P. A. Z. *Chem. Rev.* **2002**, *102*, 3667. (c) Endres, F. *ChemPhysChem* **2002**, *3*, 144. (d) Wilkes, J. S. *Green Chem.* **2002**, *4*, 73. (e) Sheldon, R. *Chem. Commun.* **2001**, 2399. (f) Welton, T. *Chem. Rev.* **1999**, *99*, 2071.
- (2) (a) Kubo, W.; Kitamura, T.; Hanabusa, K.; Wada, Y.; Yanagida, S. *Chem. Commun.* **2002**, 374. (b) Bonhôte, P.; Dias, A. P.; Papageorgiou, N.; Kalyanasundaram, K.; Grätzel, M. *Inorg. Chem.* **1996**, *35*, 1168.
- (3) (a) Visser, A. E.; Holbrey, J. D.; Rogers, R. D. *Chem. Commun.* **2001**, 2484. (b) Chun, S.; Dzyuba, S. V.; Bartsch, R. A. *Anal. Chem.* **2001**, *73*, 3737. (c) Visser, A. E.; Swatloski, R. P.; Reichert, W. M.; Griffin, S. T.; Rogers, R. D. *Ind. Eng. Chem. Res.* **2000**, *39*, 3596. (d) Visser, A. E.; Swatloski, R. P.; Rogers, R. D. *Green Chem.* **2000**, *2*, 1.
- (4) (a) Zhang, J.; Bond, A. M. *Anal. Chem.* **2003**, *75*, 6938. (b) Zhang, J.; Bond, A. M.; Belcher, W. J.; Wallace, K. J.; Steed, J. W. *J. Phys. Chem. B* **2003**, *107*, 5777. (c) Zhang, J.; Bond, A. M. *Anal. Chem.* **2003**, *75*, 2694. (d) Hultgren, V. M.; Mariotti, A. W. A.; Bond, A. M.; Wedd, A. G. *Anal. Chem.* **2002**, *74*, 3151.
- (5) (a) Carter, M. T.; Osteryoung, R. A. *J. Electrochem. Soc.* **1994**, *141*, 1713. (b) Tang, J. S.; Shimizu, K.; Osteryoung, R. A. *Inorg. Chem.* **1992**, *31*, 2328. (c) Carter, M. T.; Osteryoung, R. A. *J. Electrochem. Soc.* **1992**, *139*, 1795. (d) Carter, M. T.; Hussey, C. L.; Strubinger, S. K. D.; Osteryoung, R. A. *Inorg. Chem.* **1991**, *30*, 1149.
- (6) Lagrost, C.; Carrié, D.; Vaultier, M.; Hapiot, P. *J. Phys. Chem. A* **2003**, *107*, 745.
- (7) Bard, A. J.; Faulkner, L. R. *Electrochemical Methods*, 2nd ed.; Wiley: New York, 2001.
- (8) (a) AlNashef, I. M.; Leonard, M. L.; Matthews, M. A.; Weidner, J. W. *Ind. Eng. Chem. Res.* **2002**, *41*, 4475. (b) AlNashef, I. M.; Leonard, M. L.; Kittle, M. C.; Matthews, M. A.; Weidner, J. W. *Electrochem. Solid State Lett.* **2001**, *4*, D16.
- (9) Sweeny, B. K.; Peters, D. G. *Electrochem. Commun.* **2001**, *3*, 712.
- (10) Scholz, F.; Meyer, B. In *Electroanalytical Chemistry*; Bard, A. J., Ed.; Marcel Dekker: New York, 1998; Vol. 20, p1.
- (11) Bond, A. M. *Broadening electrochemical horizons: principles and illustration of voltammetric and related techniques*; Oxford University Press: Oxford, 2002.
- (12) (a) Hogan, C. F.; Bond, A. M.; Neufeld, N. K.; Connelly, N. G.; Llamas-Rey, E. *J. Phys. Chem. A* **2003**, *107*, 1274. (b) Connelly, N. G.; Hassard, K. A.; Dunne, B. J.; Orpen, A. G.; Raven, S. B.; Carriedo, G. A.; Riera, V. J. *Chem. Soc., Dalton Trans.* **1988**, 1623. (c) Bombin, F.; Carriedo, G. A.; Miguel, J. A.; Riera, V. J. *Chem. Soc., Dalton Trans.* **1981**, 2049.
- (13) (a) Bond, A. M.; Colton, R. *Coord. Chem. Rev.* **1997**, *166*, 161. (b) Vallat, A.; Person, M.; Roullier, L.; Laviron, E. *Inorg. Chem.* **1987**, *26*, 332. (c) Bond, A. M.; Grabaric, B. S.; Jackowski, J. J. *Inorg. Chem.* **1978**,

- 17, 2153. (d) Wimmer, F. L.; Snow, M. R.; Bond, A. M. *Inorg. Chem.* **1974**, *13*, 1617.
- (14) Carriedo, G. A.; Riera, V.; Santamaria, J. J. *Organomet. Chem.* **1982**, *234*, 175.
- (15) Chatt, J.; Watson, H. R. *J. Chem. Soc.* **1961**, 4980.
- (16) Sawyer, D. T.; Sobkowiak, A.; Roberts, J. L., Jr. *Electrochemistry for Chemists*, 2nd ed.; Wiley: New York, 1995.
- (17) Bonhôte, P.; Dias, A. P.; Papageorgiou, N.; Kalyanasundaram, K.; Grätzel, M. *Inorg. Chem.* **1996**, *35*, 1168.
- (18) MacFarlane, D. R.; Meakin, P.; Sun, J.; Amini, N.; Forsyth, M. *J. Phys. Chem. B* **1999**, *103*, 4164.
- (19) Stojanovic, R. S.; Bond, A. M. *Anal. Chem.* **1993**, *65*, 56.
- (20) Rudolph, M.; Reddy, D. P.; Feldberg, S. W. *Anal. Chem.* **1994**, *66*, 589A.
- (21) Bond, A. M.; Feldberg, S. W.; Miao, W. J.; Oldham, K. B.; Raston, C. L. *J. Electroanal. Chem.* **2001**, *501*, 22.
- (22) Majda, M. In *Molecular Design of Electrode Surfaces*; Murray, R. W., Ed.; J. Wiley & Sons: New York, 1992; pp 159–206 and references therein.
- (23) Schröder, U.; Oldham, K. B.; Myland, J. C.; Mahon, P. J.; Scholz, F. *J. Solid State Electrochem.* **2000**, *4*, 314.
- (24) (a) Pombeiro, A. J. L.; Guedes da Silva, M. F. C.; Lemos, M. A. N. D. A. *Coord. Chem. Rev.* **2001**, *219–221*, 53. (b) Evans, D. H.; O'Connell, K. M. In *Electroanalytical Chemistry*; Bard, A. J., Ed.; Marcel Dekker: New York, 1986; Vol. 14, p113.
- (25) Bond, A. M.; Colton, R.; Marken, F.; Walter, J. N. *Organometallics* **1997**, *16*, 5006.
- (26) Levine, I. N. *Physical Chemistry*, 5th ed.; McGraw-Hill: Boston, 2002.
- (27) See for example: Bae, B.; Park, J. E.; Kim, Y.; Park, J. T.; Suh, I. *Organometallics* **1999**, *18*, 2513.
- (28) Kadish, K. M.; Ding, J. Q.; Malinski, T. *Anal. Chem.* **1984**, *56*, 1741.
- (29) Stojanovic, R. S.; Bond, A. M. *Anal. Chem.* **1993**, *65*, 56.